

# Enhancement on the generation of sampled phase-only holograms

P. W. M. Tsang<sup>1,\*</sup>, Y. T. Chow<sup>1</sup>, and T.-C. Poon<sup>2</sup>

<sup>1</sup>*Department of Electronic Engineering, City University of Hong Kong, Hong Kong, Special Administrative Region (SAR), China*

<sup>2</sup>*Bradley Department of Electrical and Computer Engineering, Virginia Tech, Blacksburg, VA 24061, USA*

*\*Corresponding author: eewmts@cityu.edu.hk*

Received March 11, 2015; accepted April 23, 2015; posted online May 25, 2015

Past research has demonstrated that if the intensity image of an object is uniformly down-sampled and converted into a Fresnel hologram, the phase component alone will be sufficient to reconstruct the source image. However, due to down-sampling, the edge and line patterns are degraded heavily. In this Letter, we propose an enhancement on the parent method by incorporating an adaptive down-sampling lattice. A hologram generated with our proposed method, which is referred to as the edge-enhanced sampled phase-only hologram, preserves favorable visual quality on both the shaded regions as well as the edge patterns of the object image.

*OCIS codes: 090.1995, 090.1760, 090.0090.*

*doi: 10.3788/COL201513.060901.*

A digital hologram is a complex image that records the optical waves emitted from a three-dimensional (3D) object scene. In the last decade lots of research have been conducted on the development of fast methods for generating<sup>[1-5]</sup> and processing<sup>[6,7]</sup> digital holograms. In general terms, a digital hologram is a complex image comprising of a pair of orthogonal components (e.g., the magnitude and the phase components). In the past, reconstructing a complex holographic image requires each orthogonal component to be displayed with an individual spatial light modulator (SLM)<sup>[8-10]</sup>, which in itself can only present the phase or the magnitude information. Despite the effectiveness of this approach, integrating a pair of SLMs requires precise alignment of all the constituting optical accessories. To overcome these problems, a lot of research has been conducted in the generation of phase-only holograms (POHs). A POH can reconstruct the object image it represented with the phase component of the hologram alone, so that the hologram can be displayed with a single phase-only SLM. On the downside, the quality of the reconstructed image of a POH is degraded as compared with that of a full complex hologram. One of the major goals of research works in the investigation of POHs is to reduce the degradation caused by the removal of the magnitude component. Some of the successful attempts that have been made in recent years are outlined as follows, and summarized in Table 1. In Refs. [11-13], the two components of a double-phase hologram<sup>[14]</sup> are displayed at separate positions of a single SLM, and their diffracted waves are merged with a grating at the focused plane. In fact such spatial division framework can also be applied in integrating the real and the imaginary components of a complex hologram<sup>[15]</sup>. These approaches are difficult to implement as they require complicated setup and precise optical alignment which are tedious to realize in practice. A better solution is to convert the complex hologram into

a POH based on the Gerchberg-Saxton (GS) algorithm<sup>[16]</sup>, or the iterative Fresnel transform<sup>[17]</sup>. Both algorithms derive a pure POH through multiple rounds of computations, so that the reconstructed image will ultimately match to a given planar image. On the downside, the POH generated with such an approach is computationally intensive, and not suitable for handling image with multiple depth planes. Fast noniterative generation of POHs based on complex amplitude modulation and optical filtering has been proposed<sup>[18]</sup>. Another fast method, known as the “one-step phase retrieval (OSPR) process” which does not involve optical filtering, is reported<sup>[19]</sup> for generating a POH. In this approach, the source image is added with a random phase mask, and converted into a complex hologram. The phase component of the hologram is retained as the POH. However, the reconstructed images of the OSPR hologram is noisy and multiple holograms representing the same source image added with different random phase masks have to be generated to lower the speckle noise, hence increasing the amount of computation. In Refs. [20,21], a complex digital Fresnel hologram is directly converted into a POH through error diffusion<sup>[22]</sup>. The method can also be applied in embedding large amount of image data into the hologram<sup>[23,24]</sup>. Despite the success, the brightness of the reconstructed image is relatively lower, and a stronger illumination is needed. Recently, Tsang and Poon<sup>[25]</sup> has proposed the sampled phase-only hologram (SPOH) to overcome the aforementioned problems. The source image is first down-sampled with a uniform grid-cross lattice, and converted into a complex hologram. A POH is obtained by forcing the magnitude of each hologram pixel to a constant value. Reconstructed images of the SPOH are bright and visually appealing, but due to the down-sampling process, the line patterns are heavily fragmented and degraded. From Table 1, we can infer that all the methods have their pros and cons. A good

**Table 1.** Comparison of Several Modern Methods for Generating POHs

Method	Quality of Reconstructed Image/Advantages	Disadvantages
Spatial multiplexing <sup>[11-13,15]</sup>	High/computationally efficient	Only half of the display area is utilized Complicated optical setting involving high-resolution grating
GS or iterative Fresnel transform <sup>[16,17]</sup>	High/computationally intensive	Computationally intensive Suitable for 3D scenes comprising of small number of plane images
Complex modulation <sup>[18]</sup>	High/computationally efficient	Requires optical filtering
OSPR <sup>[19]</sup>	Good/computationally intensive	Reconstructed image contaminated with noise Requires generation of multiple hologram frames to attenuate the noise
Error diffusion <sup>[20,21]</sup>	High/computationally efficient	Intensity of reconstructed image is low
SPOH <sup>[25]</sup>	Good/computationally efficient	Lines and edge patterns are degraded

compromise between quality of the reconstructed image, computation efficiency, and complexity of the optical system is attained with the SPOH method.

In this work, we explore whether the generation of the SPOH can be further improved so that the lines and edge patterns of the reconstructed image can be preserved with higher fidelity, while maintaining the advantages of low complexity and high computation efficiency. To this end, we have proposed a method that employs a sampling scheme that is adaptive to the content of the image represented in the hologram. A POH generating by the proposed method is referred to as the edge-enhanced sampled phase-only hologram (EESPOH).

To begin with, the following terminology is adopted. The intensity of an object point at location  $(x, y)$  is represented by the image  $I(x, y)$ , and the axial distance of the object point to the hologram is denoted by variable  $w_{x,y}$ . Our proposed method can be divided into two stages as illustrated in Fig. 1, and described in the following.

Prior to the generation of the POH, the intensity image of the object is down-sampled by lattice  $D(x, y)$  given by

$$I_D(x, y) = \begin{cases} I(x, y) & D(x, y) = 1 \\ 0 & \text{otherwise} \end{cases}. \quad (1)$$

The down-sampling lattice,  $D(x, y)$ , is derived from the union of a uniform grid-cross pattern  $D_U(x, y)$ , and an

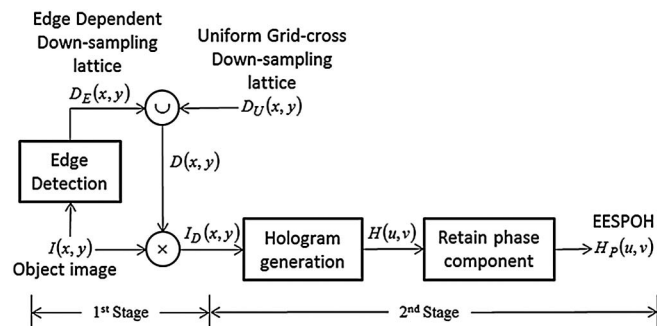


Fig. 1. Proposed method for generating the EESPOH.

edge-dependent pattern  $D_E(x, y)$  that is associated with the edges of the object image as

$$D(x, y) = D_U(x, y) \cup D_E(x, y). \quad (2)$$

In  $D_U(x, y)$ , each data point is assigned a value of unity if any one of Eqs. (3)–(5) is satisfied. Otherwise, the data point will be set to zero

$$x \bmod M \times y \bmod M = 0 \quad (3)$$

$$x \bmod M = y \bmod M \quad (4)$$

$$x \bmod M = M - 1 - (y \bmod M). \quad (5)$$

where  $M$  is the down-sampling factor, and ‘mod’ is the modulus operator that finds the remainder of division of one number by another. For example,  $5 \bmod 2$  gives 1. The second down-sampling  $D_E(x, y)$  is a down-sampling lattice that is adaptive to the edge patterns of the object image  $I(x, y)$ . To obtain  $D_E(x, y)$ , the object image  $I(x, y)$  is first convolved with Laplacian operator  $L(x, y)$  given by

$$I_E(x, y) = I(x, y) * L(x, y), \quad (6)$$

where  $L(x, y)$  is a  $3 \times 3$  kernel represented in

$$L(x, y)|_{-1 \leq x, y \leq 1} = \begin{cases} 1 & x = 0 \text{ or } y = 0 \\ -\frac{1}{8} & \text{otherwise} \end{cases}. \quad (7)$$

Next,  $D_E(x, y)$  is set to unity if the absolute value of  $I_E(x, y)$  is above a fixed threshold  $T$  (which reflects strong edge or line information), and zero otherwise. Hence

$$D_E(x, y) = \begin{cases} 1 & |I_E(x, y)| > T \\ 0 & \text{otherwise} \end{cases}. \quad (8)$$

In the generation of the SPOH proposed in Ref. [25], the object image is only down-sampled by the lattice  $D_U(x, y)$ , hence resulting in heavy degradation on the edge patterns. Our present proposed method supplements these lost information with adaptive sampling pattern  $D_E(x, y)$  which includes all the essential edge pixels in the object image.

In this stage, a complex hologram is generated from the down-sampled object image according to the Fresnel diffraction equation given by

$$H(u, v) \Big|_{\substack{0 \leq x < X \\ 0 \leq y < Y}} = \sum_{x=0}^{X-1} \sum_{y=0}^{Y-1} \frac{I_D(x, y) \exp(i2\pi r_{u,v;x,y}/\lambda)}{r_{u,v;x,y}}, \quad (9)$$

where  $r_{u,v;x,y} = \sqrt{((x-u)^2\delta + (y-v)^2\delta + w_{x,y}^2)}$  is the distance between an object point located at  $(x, y)$  in the 3D scene and a point  $(u, v)$  on the hologram, with  $w_{x,y}$  being the axial distance between the image and the hologram. Wavelength of the optical beam is denoted by the variable  $\lambda$ . The constant values  $X$  and  $Y$  represent the number of rows and columns of the object image, respectively, and  $\delta$  is the size of the hologram pixel assumed to be square in shape. Subsequently, we extract the phase component  $H_p(u, v)$  of hologram  $H(u, v)$  to be phase-only; therefore

$$|H_p(u, v)| = 1, \quad \text{and} \quad \arg(H_p(u, v)) = \arg(H(u, v)). \quad (10)$$

A binary planar image “star” and a continuous tone image “eye” shown in Figs. 2(a) and 2(b), respectively, are employed to illustrate our proposed method. Both images are comprising of line patterns and smooth regions, and positioned at an axial distance of 0.3 m to the hologram. The down-sampling lattices  $D_U(x, y)$ ,  $D_E(x, y)$ , and  $D(x, y)$  are derived based on the formulations as presented previously. For the sake of comparison, we first apply the existing method in Ref. [25] to compute the SPOH of the two test images based on the optical settings in Table 2. In generating the holograms, each image is only down-sampled with the grid-cross lattice  $D_U(x, y)$ , and a complex hologram is generated with Eq. (9). The SPOH is obtained from the phase component of the complex hologram. The numerical reconstructed images of the two SPOHs are shown in Figs. 3(a) and 3(b). It can be seen that in both reconstructed images, the shaded regions are well-preserved, but the continuous line patterns are severely fragmented. Next we apply our proposed method to generate the edge-enhanced SPOHs for the test images, based on the down-sampling lattice  $D(x, y)$  with identical

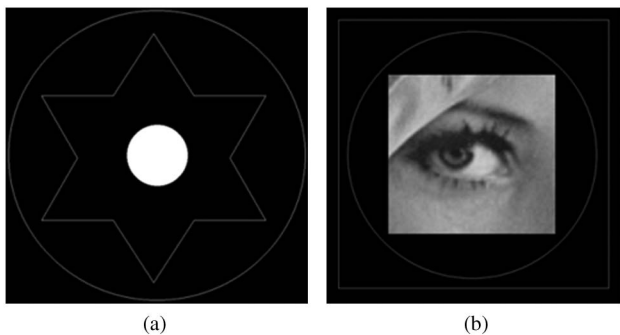


Fig. 2. Object images (a) “star” and (b) “eye”.

**Table 2.** Optical Settings for Generating the Digital Hologram

Wavelength $\lambda$	633 nm	Hologram size	2048 × 2048
Pixel size	8 $\mu\text{m}$ × 8 $\mu\text{m}$	Image size	1024 × 1024

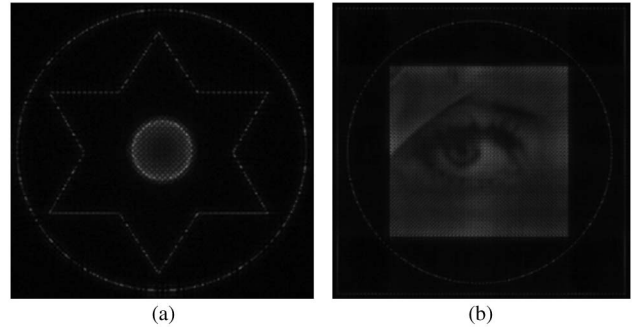


Fig. 3. Numerical reconstructed images of the SPOHs of the object images (a) “star” and (b) “eye”.

optical settings. The numerical reconstructed images are shown in Figs. 4(a) and 4(b). We observe that both the shaded regions, as well as the edge (e.g., the boundary of the square region in the “eye” image) and line patterns are preserved with good fidelity. The correlation score between the reconstructed images of the EESPOHs in Figs. 4(a) and 4(b), and the ones obtained from the complex holograms of the original images are 0.658 and 0.664, respectively, reflecting reasonable degree of similarities and also certain degradation due to the down-sampling.

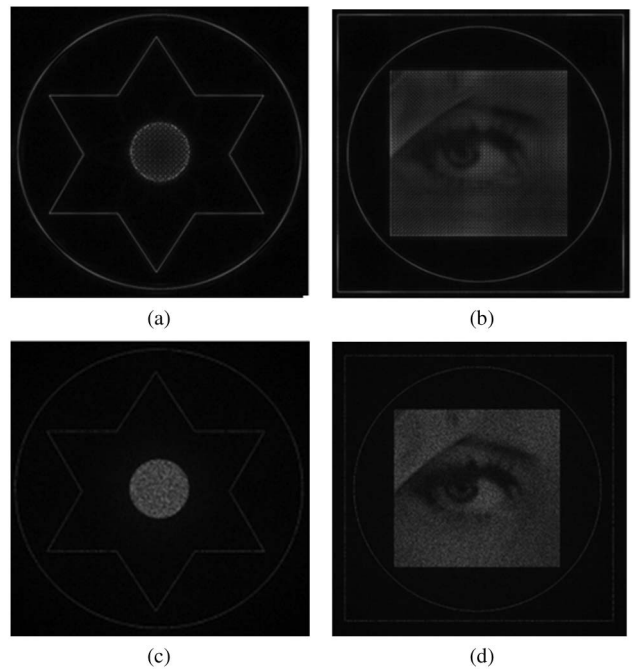


Fig. 4. Numerical reconstructed of the EESPOHs of the object images (a) “star” and (b) “eye”; numerical reconstructed images of POHs generated with random phase noise added to the original (c) “star” and (d) “eye” images.



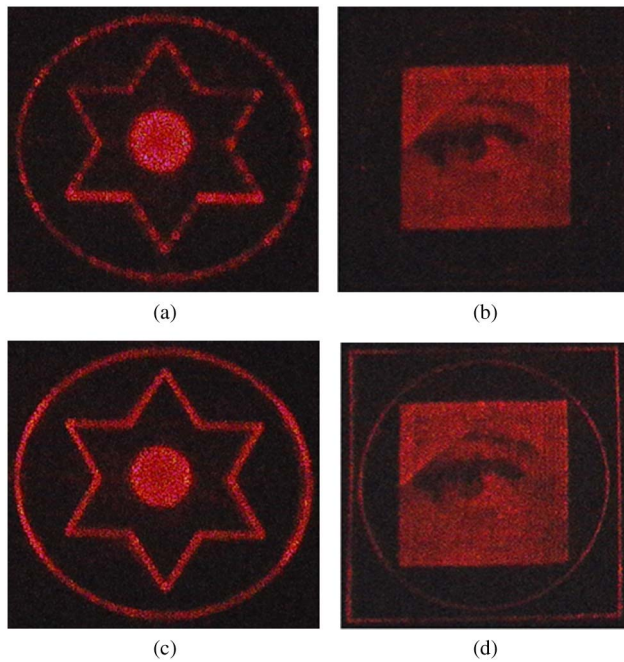


Fig. 5. Optical reconstructed images of the SPOHs of the object images (a) “star” and (b) “eye”; optical reconstructed images of the EESPOHs of the object images (c) “star” and (d) “eye”.

For the sake of comparison we also show, in Figs. 4(c) and 4(d), the numerical reconstructed images of POHs that are generated by adding random phase noise to the original image prior to the generation of the POHs (obtained by preserving only the phase component of the complex hologram). We have observed that the reconstructed images are heavily contaminated with noise, and the lines are also fragmented and weaker in appearance. Subsequently, the SPOHs and the EESPOHs are inputted to the Holoeye LCR1080 SLM. Upon illumination with a coherent plane wave, the optical reconstructed image of the hologram is formed at the focused plane, and shown in Figs. 5(a)–5(d). It can be seen that the results of the numerical and the optical reconstruction are rather similar, with the reconstructed images of the proposed method exhibiting obvious improvements over those obtained with the existing method in Ref. [25]. However, we also notice that due to the imperfection of the SLM and the optical setups, the quality of the optical reconstructed images is relatively inferior as compared with that of the numerical reconstruction results.

In conclusion, we describe an improved method for fast generation of POHs based on down-sampling of the object image. In the approach, the intensity of the object image is first down-sampled with a lattice that is composed of a uniform grid-cross and an edge-dependent lattice. Subsequently, a complex hologram is generated from the down-sampled object image, and the phase component is retained as an EESPOH. Experimental results obtained with numerical and optical reconstruction demonstrate that the reconstructed image of the EESPOH is bright, and capable of preserving good visual quality on both

the shaded regions and the edge patterns. The improvement is apparent when compared with the POHs obtained with the existing method in Ref. [25], in which case the edge and line patterns of the reconstructed images are heavily degraded. Our proposed method is also computationally efficient, as the additional overhead imposed in the generation of the hologram is attributed to the edge detection and the down-sampling process, both of which only involve small amount of arithmetic operations. These favorable outcomes suggest that our proposed method can be practically applied in the fast generation of POHs that are suitable for visual display. Further research can be conducted to explore the possibility of enhancing the reconstructed images of the EESPOHs based on edge detection schemes other than the Laplacian operator.

## References

1. P. W. M. Tsang and T.-C. Poon, *Opt. Express* **23**, 7667 (2015).
2. Y. Zhang, W. Peng, H. Chen, Y. Xu, W. Chen, and W. Xu, *Chin. Opt. Lett.* **12**, 030902 (2014).
3. S.-C. Kim and E.-S. Kim, *Opt. Express* **22**, 22513 (2014).
4. J. Weng, T. Shimobaba, N. Okada, H. Nakayama, M. Oikawa, N. Masuda, and T. Ito, *Opt. Express* **20**, 4018 (2012).
5. P. W. M. Tsang, W.-K. Cheung, T.-C. Poon, and C. Zhou, *Opt. Express* **19**, 15205 (2011).
6. P. W. M. Tsang and T.-C. Poon, *Chin. Opt. Lett.* **11**, 010902 (2013).
7. Y. Lam, W. Situ, and P. W. M. Tsang, *Chin. Opt. Lett.* **11**, 050901 (2013).
8. M. Makowski, A. Siemion, I. Ducin, K. Kakarenko, M. Sypek, A. Siemion, J. Suszek, D. Wojnowski, Z. Jaroszewicz, and A. Kolodziejczyk, *Chin. Opt. Lett.* **9**, 120008 (2011).
9. M.-L. Hsieh, M.-L. Chen, and C.-J. Cheng, *Opt. Eng.* **46**, 070501 (2007).
10. R. Tudela, E. Martín-Badosa, I. Labastida, S. Vallmitjana, I. Juvells, and A. Carnicer, *J. Opt. A* **5**, S189 (2003).
11. X. Li, Y. Wang, J. Liu, J. Jia, Y. Pan, and J. Xie, in *Digital Holography and Three-Dimensional Imaging* (OSA, 2013), paper DTh2A.3.
12. S. Reichelt, R. Häussler, G. Fütterer, N. Leister, H. Kato, N. Usukura, and Y. Kanbayashi, *Opt. Lett.* **37**, 1955 (2012).
13. H. Song, G. Sung, S. Choi, K. Won, H. Lee, and H. Kim, *Opt. Express* **20**, 29844 (2012).
14. C. Hsueh and A. Sawchuk, *Appl. Opt.* **17**, 3874 (1978).
15. J.-P. Liu, W. Hsieh, T.-C. Poon, and P. W. M. Tsang, *Appl. Opt.* **50**, H128 (2011).
16. R. W. Gerchberg and W. O. Saxton, *Optik* **35**, 237 (1972).
17. J. Yeom, J. Hong, J.-H. Jung, K. Hong, J.-H. Park, and B. Lee, *Chin. Opt. Lett.* **9**, 120009 (2011).
18. X. Li, J. Liu, J. Jia, Y. Pan, and Y. Wang, *Opt. Express* **21**, 20577 (2013).
19. E. Buckley, in *Society for Information Display* (2008) pp. 1074.
20. P. W. M. Tsang, A. S. M. Jiao, and T.-C. Poon, *Opt. Express* **22**, 5060 (2014).
21. P. W. M. Tsang and T.-C. Poon, *Opt. Express* **21**, 23680 (2013).
22. R. W. Floyd and L. Steinberg, *Proc Soc. Info. Disp.* **17**, 75 (1976).
23. P. W. M. Tsang and T.-C. Poon, *Chin. Opt. Lett.* **12**, 060017 (2014).
24. P. W. M. Tsang, Y. T. Chow, and T.-C. Poon, *Opt. Commun.* **341**, 188 (2015).
25. P. W. M. Tsang, Y. T. Chow, and T.-C. Poon, *Opt. Express* **22**, 25208 (2014).